Solitary Modes of Bacterial Culture in a Temperature Gradient

H. Salman, A. Zilman, C. Loverdo, M. Jeffroy, and A. Libchaber

Center for Studies in Physics and Biology, The Rockefeller University, New York, New York 10021, USA

(Received 8 February 2006; published 11 September 2006)

We study the behavior of a bacterial culture in a one-dimensional temperature gradient. The bacteria first accumulate near their natural temperature due to thermotaxis. The maximum of the bacterial density profile then drifts to lower temperature with a velocity proportional to the initial concentration of bacteria (typical velocity 0.5 μm/sec). Above a critical concentration of 10^8 cells/cm^3, a new mode develops from the initial accumulation in the form of a sharp pulse moving at a faster velocity ($\sim$3.5 μm/sec). The time of development of this mode diverges as the concentration approaches its critical value. This mode is a result of a positive feedback mechanism provided by interbacterial communication. A theoretical model shows good agreement with the experimental results.

DOI: 10.1103/PhysRevLett.97.118101 PACS numbers: 87.17.Jj, 87.17.Aa, 87.18.Hf

Sensing changes in the environment is a fundamental property of living organisms. It allows them to respond and adapt to their new surroundings. In the case of bacteria the response can take different forms, such as modifying their gene-expression profile [1], or altering their swimming pattern [2–6]. In this work we study the response of *E. coli* bacteria to a spatial variation of temperature, i.e., to a temperature gradient. We examine the temporal behavior of the culture under the temperature gradient and how it is affected by the bacterial density.

Starting from a uniform concentration, we observe an initial accumulation of the bacteria, which subsequently propagate down the temperature gradient (Fig. 2). This dynamical mode, in the form of high cell density pulse, is a result of the combined effect of the gradients of temperature and nutrients. Thermotaxis, the temperature-sensing ability, drives the bacteria towards their natural temperature and causes the initial accumulation. The subsequent propagation is due to faster food depletion at the accumulation region and chemotactic response. The direction of propagation is determined by the gradient of nutrients created due to lower bacterial metabolism at low temperature. Above a critical initial cell density, this mode becomes unstable to a new large-amplitude and fast pulse (Fig. 3). The bifurcation to this new mode is a result of a chemical interaction among the bacteria, which are attracted to an attractant that they themselves secrete, thereby amplifying the initial density increase [7].

The bacteria sense temperature changes using the chemical-sensing receptors Tar, Tsr, Trg, and Tap [8,9], which are also involved in chemotaxis. The bacteria respond by changing their swimming pattern. A favorable change in the environment, whether in space or in time, is translated into a reduction in the tumbling frequency of the bacteria and vice versa [2,4,6,10]. The temperature can cause a conformational change in these receptors that affect their binding affinity [11,12]. Each receptor, though, reacts differently to different temperature changes [9–14].

To study the behavior of the bacteria in a one-dimensional space, we have developed the experimental setup described in Fig. 1. Our results show that upon applying a temperature gradient (10 to 45 °C) along the channels, the bacteria are depleted from the cold and hot regions, while their concentration increases around 30 °C

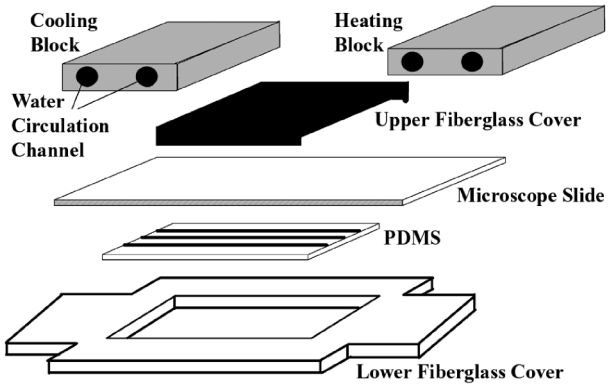

FIG. 1. The experimental setup: a set of narrow channels (0.07 × 0.002 cm), 3 cm long, microfabricated with polydimethyl-siloxane (PDMS). The 0.02 cm depth inhibits convection [25]. This was also verified using 2 μm size polysterene beads. Typical temperatures applied to the ends of the channels, 10 °C on the cold edge and 45 °C on the hot one. The bacterial culture, the wild-type RP437 or the mutant HCB2415 [7] *E. coli*, was launched from a frozen glycerol stock and grown overnight at 30 °C, in a M9 minimal medium supplemented with 1% casamino acids and 4% glucose, to an O.D.$_{600\ \mathrm{nm}}$ of 0.2 to 0.4 (2–4 × 10^8 cells/cm^3). Prior to filling the channels, the bacteria were concentrated and resuspended in fresh medium that was kept also at 30 °C. The bacteria were visualized by fluorescence microscopy using YFP (or GFP in the case of the mutant) gene inserted as a plasmid. The observation chamber was mounted on an inverted Zeiss microscope, Axiovert 35 M, while the heating and cooling blocks were connected to water baths. Imaging was done using two objectives, the 10× for single cell counting, and the 2.5× for wide range profiling, by collective fluorescence measurements. The initial cell density in each channel was estimated by counting the number of cells per unit volume. Images of the bacteria were acquired using an Apogee cooled CCD (Apogee Instruments Inc.).

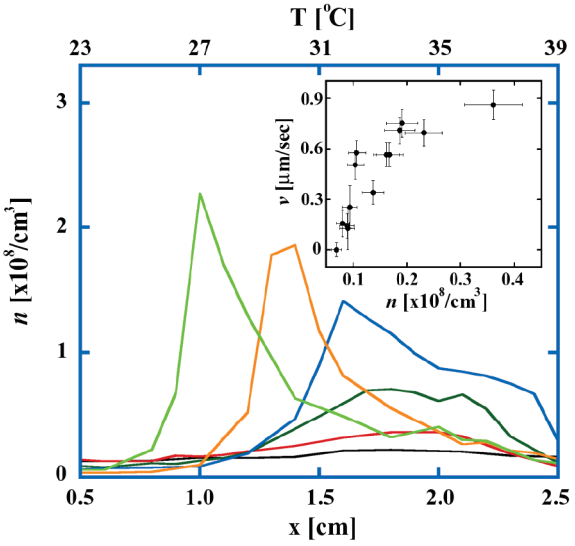

FIG. 2 (color). Distribution of the bacterial concentration at different times in the low concentration regime: before applying the gradient (black), 45 ± 10 min (red), 85 ± 10 min (dark green), 145 ± 10 min (blue), 204 ± 15 min (orange), and 255 ± 10 min (light green). Lower x axis: position in the channel measured from the edge of the cooling block. Upper x axis: corresponding temperature. Inset: average drift velocity of the peak v as a function of the initial cell density n. Measurements were carried out by counting the bacteria at different locations through the channel.

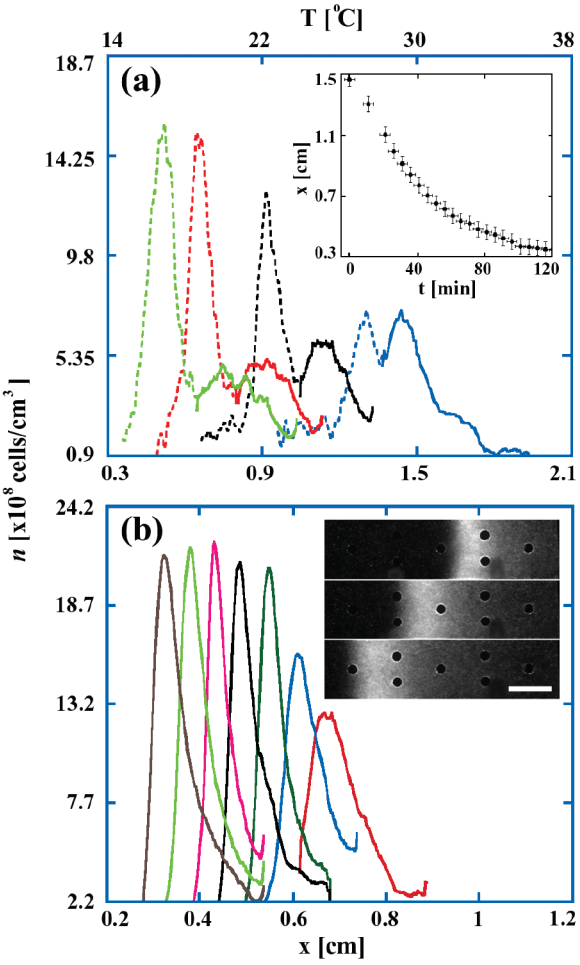

FIG. 3 (color). Fluorescence measurements of the emergence of the second mode. (a) Evolution of the second mode from the initial accumulation, with 6 minutes separation between consecutive measurements. First measurement taken 50 minutes after applying the gradient. The solid line represents the first mode, while the dashed line denotes the second mode. The inset shows the position of the second mode in time until it reaches a full rest at 14 °C, where bacterial metabolism and flagella velocity is strongly reduced. (b) Propagation of the second mode upon switching to a 30 °C uniform temperature, with 3 minutes separation between consecutive measurements. The images of the last three peaks are shown in the inset. Scale bar: 0.05 cm. The black spots in the images are PDMS pillars that act as supports in the channel.

(Fig. 2). This accumulation takes about 30 minutes. It was previously observed under similar conditions by Oosawa group [10]. Beyond that time, a steady motion of the peak towards the cold end of the channel is observed. It is caused by a higher rate of nutrient depletion at the warm side due to higher bacterial metabolism, which creates a gradient of nutrients that triggers the chemotactic response of the bacteria. As the initial bacterial concentration increases, the cell density in the peak becomes higher and the local depletion of the food becomes faster. This increases the local gradient of nutrients [7,15–19]. Therefore, the velocity of the peak increases with the bacteria's initial concentration up to a maximum velocity of $\sim 1\ \mu\mathrm{m}/\mathrm{sec}$ (Fig. 2, inset).

Above a critical initial cell density ($n_c = 10^8$ cells/cm^3), a drastic change in the collective behavior of the bacteria is observed. At this concentration, the initial accumulation of bacteria evolves into a sharp peak solitary mode. The transition is fast (of the order of 5 min) relative to the first mode accumulation time [Fig. 3(a)]. The time needed for the second mode to develop increases as the concentration decreases and diverges close to the critical cell density (Fig. 4). The concentration of bacteria in the new mode is an order of magnitude higher and allows measurement by fluorescence [Fig. 3(b), inset]. The new mode propagates towards the cold end of the channel with a much higher initial velocity (maximum $\sim 3.5\ \mu\mathrm{m}/\mathrm{sec}$). However, the velocity of the peak decreases as it explores lower temperature [Fig. 3(a), inset].

This second mode appears only beyond a critical cell density. Therefore, if this mode develops due to chemical signaling between bacteria, its persistence should not depend on the temperature gradient. Indeed, when switching to a 30 °C uniform temperature, the peak sharpened even more and continued at a velocity of $\sim 3.5\ \mu\mathrm{m}/\mathrm{sec}$ [Fig. 3(b) and Fig. 5, inset). Moreover, switching the direction of the temperature did not stop the propagation

of the peak until it reached ~40 °C (results not shown). Based on previous studies [7,16], we presume that the cell-cell signaling is mediated by the secretion of and attraction to glycine. The initial accumulation leads to a local increase in the excreted glycine concentration, which in turn attracts nearby bacteria. Thus, a positive feedback is created that amplifies the accumulation.

The amino acid glycine is an attractant detected by the chemoreceptor Tsr, [11,20]. Therefore, to test our assumption that the second mode emerges due to secretion and sensing of glycine by the Tsr receptor, we tested the behavior of a mutant strain of the bacterium with the Tsr receptor deleted [7]. Indeed, this mode disappeared for cell densities as high as 2.5×10^8 cells/cm^3 (Fig. 4). Above this new critical concentration [21] the mode reappeared similar to that of the wild type but with a longer delay (Fig. 4, inset).

In additional tests, we saturated the medium with one of the two amino acids, glycine, or *L*-serine, which is also detected by Tsr. At a very high concentration of a chemical attractant, its receptor will be saturated. Our results show that the appearance of the new mode was prevented by the addition of 10 mM glycine or *L*-serine to the medium. As a control we used 10 mM of *L*-aspartate, which interacts with another chemoreceptor (Tar) and found no effect. These results indicate that cell-cell signaling through glycine plays a major role in the appearance of the second mode, although other molecules might be involved as well.

The spatial evolution of the bacterial density, coupled to the attractant production, food consumption, and spatial diffusion of the bacteria and the nutrients, can be described by the modified Keller-Segel equations [7,17,22]:

$$\frac{\partial n}{\partial t} = D_b \nabla^2 n - k_c \nabla(n \nabla c) - k_f \nabla(n \nabla f),$$
$$\frac{\partial c}{\partial t} = D_c \nabla^2 c + J n(x,t) - \varepsilon c,$$
$$\frac{\partial f}{\partial t} = D_f \nabla^2 f - b n(x,t),$$

where $n(x,t)$ is the density of the bacteria, $c(x,t)$ is the density of the attractant, and $f(x,t)$ is the density of the rest of the nutrients. The coefficients k_c and k_f reflect the strength of the chemotactic response to the attractant and nutrient gradient, respectively, and D_b is the effective diffusion coefficient of the bacteria $D_b = l^2\omega$, l is the mean run length, and ω is the average tumbling frequency [17]. The coefficients J and b are the rate of attractant production and nutrient consumption, respectively; ϵ is the degradation rate of the extracellular attractant. The coefficients in the above equations depend on the nutrients and the attractant densities. It has been found that the chemotactic sensing ability of the bacteria sharply decreases below a certain attractant concentration, c_0 [20], which is specific to the attractant. To account for this effect we assume that $k_c = c^2/(c_0^2 + c^2)$ [23].

Numerical solution of the modified Keller-Segel equations is presented in Fig. 5. As initial conditions we use the Gaussian shaped density profile and the preexisting nutrient gradient [24]. The solution shows that above a critical bacterial density, a sharp peak forms that subsequently propagates along the preexisting gradient of nutrients. The

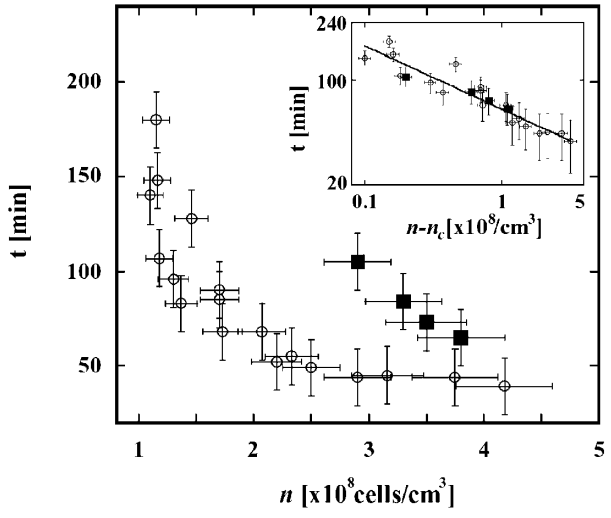

FIG. 4. The development time of the second mode as a function of the initial cell density n. Wild-type bacteria (empty circles) and mutant with deleted Tsr receptor (full squares). Inset: log-log plot of the development time as a function of n-n_c, where n_c is the critical cell density 10^8 cells/cm^3 for the wild type and 2.7×10^8 cells/cm^3 for the mutant [21]. Line: a power low fit with an exponent of -0.4.

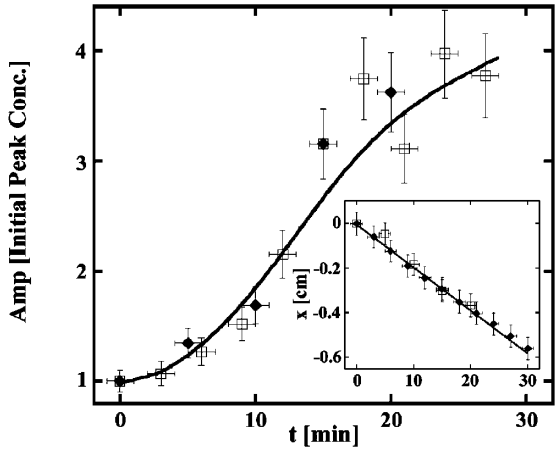

FIG. 5. Comparison between the numerical solution and the data from two different experiments. The line depicts the solution to the Keller-Segal equations. Origin of time is the time of switching to 30 °C. The amplitude is given relative to the concentration in the peak at $t = 0$. The inset depicts the position of the peak in time. Parameters used in the numerical solution: $D_b = 1.7 \times 10^{-6}$ cm^2/sec, $D_c = D_f = 8 \times 10^{-5}$ cm^2/sec, $k_c = k_f = 1.2 \times 10^{-20}$ cm^5/sec [26], $J = 4 \times 10^5$/bacterium/sec [7], $\varepsilon = 0.005$ mole/sec, $c_0 = 10^{-5}$ M [20].

qualitative shape of the solution is robust to the changes of the parameters values. It is in good agreement with the experimental data for the growth in the amplitude and the change in the peak's position (Fig. 5).

Existence of a critical bacterial density above which the sharp peak mode appears can be understood by considering the second of the Keller-Segel equations. It follows that for slowly changing profiles, the average local density of attractant c is $c = nJ/\varepsilon$. Here n is the average local concentration of bacteria. The chemotactic response, as reflected by k_c, is significant only for $c > c_0$ and hence, for $n > c_0\varepsilon/J$. Below this critical concentration of bacteria, the effective attraction is not high enough to trigger the bacterial aggregation. We also note that the specific value of the critical cell density for the appearance of the second mode (1×10^8 cells/cm^3) depends among other things on the size of the system. The initial cell accumulation starts drifting towards colder temperature early in the process. Intercell communication is reduced at colder temperatures. Thus, the second mode cannot appear if it is not triggered before the peak reaches the low temperature region. The drift velocity of the accumulation peak is determined primarily by the gradient of nutrients and the chemotactic sensitivity of the bacteria at a given temperature. The higher velocity of the second mode is attributed to the high cell density (an order of magnitude higher) in the peak, which depletes the food locally much faster.

In summary, we have observed and modeled the formation and propagation of a novel collective mode of bacterial dynamics. We have shown that this mode develops above a critical cell density, and that it grows from an initial bacterial accumulation initiated by thermotaxis. This mode is the result of bacteria secreting their own attractant, providing a positive feedback mechanism for amplification of local density increase. The density dependence of the transition threshold is explained by the low sensitivity of the bacteria at low attractant concentration. If the rate of the attractant production and the chemotactic response to the attractant gradient are high enough to overcome the diffusion out of the accumulation region, a sharp peak grows exponentially. Our results show that secretion of glycine and attraction to it is important for the collective behavior of the bacteria. Yet, as mentioned above, it seems that there are other factors that contribute as well. To identify these factors, more work and mutant screening are required, which we are attempting at the present time.

We would like to thank the lab of Robert H. Austin for the gift of mutant bacteria.

[1] B. Muller-Hill, *The lac Operon: A Short History of a Genetic Paradigm* (Walter de Gruyter, New York, 1996).
[2] H. C. Berg, *E. coli in Motion* (Springer, New York, 2003).
[3] J. Adler, Science **234**, 40 (1976).
[4] U. Alon *et al.*, EMBO J. **17**, 4238 (1998).
[5] W. Shi, M. J. Lentz, and J. Adler, J. Bact. **175**, 5785 (1993).
[6] Y. Imae, T. Mizuno, and K. Maeda, J. Bact. **159**, 368 (1984).
[7] S. Park *et al.*, Proc. Natl. Acad. Sci. U.S.A. **100**, 13 910 (2003).
[8] Y. Imae, *Sensing and Response in Microorganisms*, edited by M. Eisenbach and M. Balaban (Elsevier, New York, 1985), p. 73.
[9] T. Nara, L. Lee, and Y. Imae, J. Bact. **173**, 1120 (1991).
[10] K. Maeda, Y. Imae, J. I. Shioi, and F. Oosawa, J. Bact. **127**, 1039 (1976).
[11] K. Maeda and Y. Imae, Proc. Natl. Acad. Sci. U.S.A. **76**, 91 (1979).
[12] T. Mizuno and Y. Imae, J. Bact. **159**, 360 (1984).
[13] S. Nishiyama *et al.*, J. Bact. **179**, 6573 (1997).
[14] S. Nishiyama, I. N. Maruyama, M. Homma, and I. Kawagishi, J. Mol. Biol. **286**, 1275 (1999).
[15] E. O. Budrene and H. C. Berg, Nature (London) **349**, 630 (1991).
[16] E. O. Budrene and H. C. Berg, Nature (London) **376**, 49 (1995).
[17] M. P. Brenner, L. S. Levitov, and E. O. Budrene, Biophys. J. **74**, 1677 (1998).
[18] J. Adler, Science **153**, 708 (1966).
[19] R. Nossal, Exp. Cell Res. **75**, 138 (1972).
[20] R. Mesibov and J. Adler, J. Bact. **112**, 315 (1972).
[21] The new critical concentration for the mutant strain was determined to be 2.7×10^8 cells/cm^3, by fitting the new results to the power law fit of the wild-type strain.
[22] E. F. Keller and L. A. Segel, J. Theor. Biol. **30**, 225 (1971).
[23] The results are not sensitive to the exact functional dependence of k_c. We have also included the saturation of the chemotactic response at high attractant concentration, which has been observed in our experiments for glycine and *L*-serine, and the decrease in metabolic nutrient consumption at low nutrient concentration.
[24] The Gaussian shaped density profile is due to the thermotaxis, and the nutrient gradient is due to the higher metabolic rates at higher temperature. Also, we do not explicitly take the temperature dependence in the coefficients.
[25] D. Braun and A. Libchaber, Phys. Rev. Lett. **89**, 188103 (2002).
[26] H. C. Berg and D. A. Brown, Nature (London) **239**, 500 (1972).